LETTERS
PUBLISHED ONLINE: 21 MARCH 2010 | DOI: 10.1038/NNANO.2010.42
nature nanotechnology

Identifying single nucleotides by tunnelling current

Makusu Tsutsui[1], Masateru Taniguchi[1,2]*, Kazumichi Yokota[1] and Tomoji Kawai[1,3]*

A major goal in medical research is to develop a DNA sequencing technique that is capable of reading an entire human genome at low cost[1–4]. Recently, it was proposed that DNA sequencing could be performed by measuring the electron transport properties of the individual nucleotides in a DNA molecule[5]. Here, we report electrical detection of single nucleotides using two configurable nanoelectrodes and show that electron transport through single nucleotides occurs by tunnelling. We also demonstrate statistical identification of the nucleotides based on their electrical conductivity, thereby providing an experimental basis for a DNA sequencing technology based on measurements of electron transport.

DNA is a one-dimensional polymer composed of four types of nucleotides—thymidine, guanosine, adenosine and cytidine—the sequence of which stores genetic information inherent to individual organisms. A fast, label-free approach to DNA sequencing could lead to personalized medicine and a revolution in traditional pharmaceuticals[1–4]. In the past decade, significant progress has been made in the development of single molecule techniques that can interrogate the base sequence of DNA[3–5]. A recent accomplishment involves chemically engineered α-haemolysin nanopore detectors, in which single-molecule sequencing has been demonstrated by probing transient ion-current blockade during translocation of a single-stranded DNA oligomer through a cyclodextrin-embedded biological pore[6,7]. However, system instability and limited pore-size selectivity remain unresolved issues that hinder its practical application[3,4]. Robust, configurable solid-state nanopores have thus attracted increasing interest, serving as a platform for studying the dynamics of single biomolecules passing through pores[8–11]. However, the prospects of ionic-current-based sequencing at a resolution of a single base remain a subject of debate[3,4].

Recently, an alternative approach was proposed: DNA sequencing through transverse electron transport[4,5,12–15]. With this approach it has been predicted that a single molecule sequence could be directly read (without any previous treatment such as amplification or fluorescent labelling) at speeds exceeding 400 kb per hour, by detecting the distinct transverse electrical conductivity unique to each base (associated with differences in their HOMO–LUMO gaps) as DNA passes through a nanospace between a pair of electrodes[5,12,13] (Fig. 1a). This theoretical work has inspired several groups to develop test-bed systems by embedding nanogap electrodes in a micro- or nanofluidic channel[16–19]. However, this DNA sequencing method lacks experimental verification of its single-base detection principle.

Here, we report single-molecule detection of thymidine 5′-monophosphate (TMP), guanosine 5′-monophosphate (GMP) and cytidine 5′-monophosphate (CMP) by means of electron tunnelling current measurements (Fig. 1b,c). Our results indicate that single nucleotides can be identified statistically through electron transmissivity related to their HOMO–LUMO gap, thus proving the efficiency of this DNA sequencing technology.

Our strategy for addressing single-molecule electron transport is based on observations of temporal changes in a two-probe tunnelling current I associated with trapping of nucleotides dissolved in Milli-Q water (∼5 μM) between gold nanoelectrodes for which the inter-electrode gap distance has been adjusted to the length of the nucleotides[19,20]. Briefly, the piezo-actuator was calibrated using vacuum tunnelling, and the gap set in the presence of a nucleotide solution by opening the junction 1 nm from its shorted position (Supplementary Figs S1,S2). Figure 2 shows typical I–t curves acquired for GMP at a constant d.c. bias V_b of 0.75 V. The small offset of ∼80 pA and a noise level of $\sim\pm$ 10 pA are attributable to the ionic nature of polarized GMPs in the solvent. The I–t curve is characterized by several pulses of different heights I_p. (I_p is defined as the maximum I attained by a single pulse subtracted from the base level.) Expanded views reveal pulse-like signals of different widths t_d (Fig. 2b). These characteristic signals are absent when the nanoelectrode gaps are wider than the molecular length of the nucleotides, ∼1.0 nm (Supplementary Fig. S3). Furthermore, measurements in a solvent containing no dissolved molecules resulted in featureless I–t characteristics. The rapid current rise and subsequent drops are therefore interpreted as denoting a trapping/detrapping event of single GMP molecule between the nanoelectrodes.

It is worth noting that current becomes increasingly unstable when GMP molecules are trapped (Fig. 2b). This presumably stems from atomistic motions of mobile nucleotide molecules in the electrode gaps[12,13]. In the present experimental conditions, in which the molecules are not connected to the metal electrodes via any strong chemical links, it is anticipated that even a marginal change in molecular conformation will lead to substantial fluctuations in I through modification of the electrode–molecule distance. Widening of the gap distance leads to weaker electrode–molecule electronic couplings and an accompanying drop in I. Conversely, narrowing of the gap distance leads to stronger electrode–molecule electronic couplings and an accompanying rise in I.

We explored the electron transport mechanism in single nucleotides by investigating the bias voltage dependence of I_p. The I–t measurements are extended to a bias range of $0.25 \leq V_b \leq 0.75$ V. Pulse-like signals of diverse I_p and t_d analogous to those presented in Fig. 2 are detected at the V_b conditions measured (Fig. 3a–c).

The I_p–V_b characteristics were examined by statistically analysing I pulses. Histograms were constructed from 500 samples of I_p data. The I_p histograms reveal an expansive distribution that extends for more than one order of magnitude. This is ascribable to a variation in electrode − molecule contact lengths associated with the aforementioned diverse molecular conformations of mobile GMPs in the electrode gaps. However, well-defined single peaks still appear in the I_p distributions. The single peak structures indicate preferred conformations of GMP molecules residing in the electrode gap nanospace under an electrical field, which could be due in part to nucleotide base molecule alignments along the electrostatic potential gradient induced by V_b (ref. 5).

[1]The Institute of Scientific and Industrial Research, Osaka University, 8-1 Mihogaoka, Ibaraki, Osaka 567-0047, Japan, [2]PRESTO, Japan Science and Technology Agency, Honcho, Kawaguchi, Saitama 332-0012, Japan, [3]Division of Quantum Phases & Devices, Department of Physics, Konkuk University, Seoul 143-701, Republic of Korea. *e-mail: taniguti@sanken.osaka-u.ac.jp; kawai@sanken.osaka-u.ac.jp

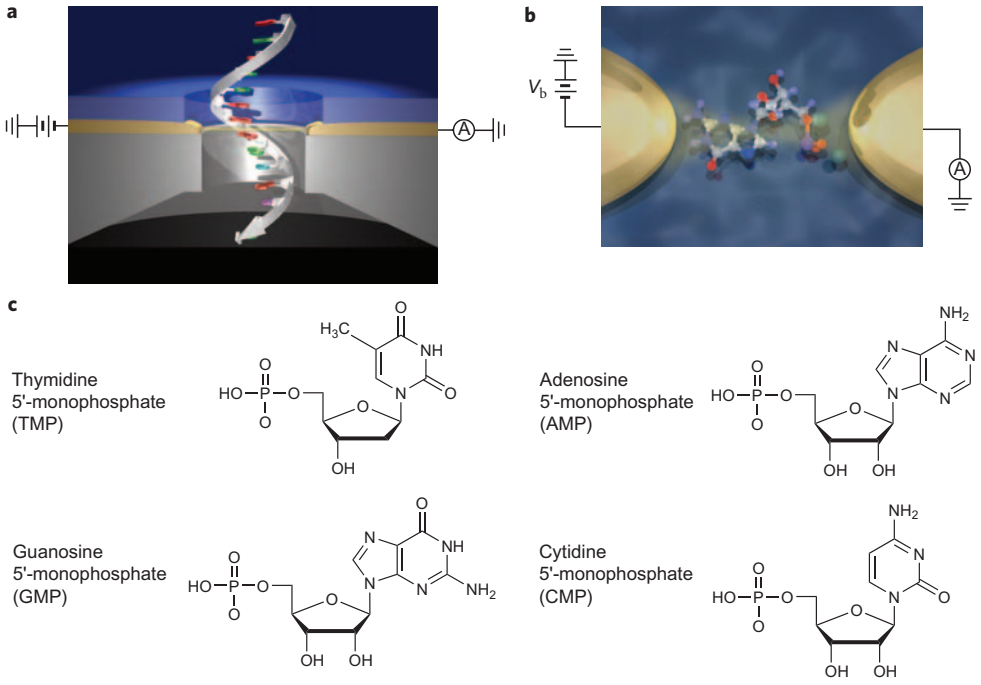

Figure 1 | Conceptual illustrations of single-nucleotide conductance measurements for DNA sequencing. a, Schematic of the new DNA sequencing method. A single-molecule DNA translocates through a nanopore. Simultaneously, a pair of nanoelectrodes fabricated at the pore edges scans the tunnelling current across each nucleotide, thereby realizing direct label-free base sequence read-out. **b**, Model depicting tunnel current measurements of a single-nucleotide molecule trapped between two gold nanoelectrodes under a d.c. bias V_b in water. **c**, Molecular structures of the nucleotides used in this study.

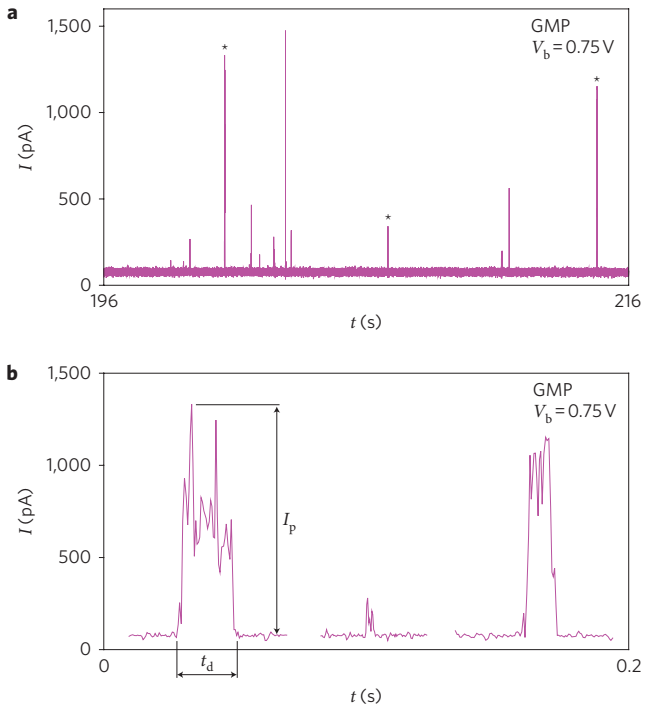

Figure 2 | I–t curves obtained for GMP at $V_b = 0.75$ V with electrode gap size adjusted to 1.0 ± 0.05 nm. a, Examples of pulse-like signals. Only a part of the curve is displayed for clear visualization; the entire data set spans over 3,000 s. Several pulse-like signals with various heights emerge randomly with time. **b**, Expanded view of the I pulses marked by asterisks in **a**. I_p and t_d are defined as the maximum height and the pulsewidth of an I pulse, respectively.

The single peak I_p, which is relevant to single molecule conductance of GMPs, with a specific conformation emerging with statistical significance in the experiments, was extracted by Gaussian fitting to the histograms and plotted as a function of V_b (Fig. 3d). The plots clearly show a linear increase of I_p with V_b. From this I_p–V_b dependence, we conclude that there is a possible electron transport mechanism occurring in the nucleotides. It is first assumed that there are non-negligible charge injection barriers at the electrode–molecule interfaces. Rough estimations with density functional theory (DFT) calculations[21] of the molecular frontier orbital levels using the B3LYP functional and 6-31G** basis set yielded an injection barrier energy of ~2.6 eV at the gold–guanine contacts (here, the Fermi level of the electrode is assumed to align with the midpoint of the molecular HOMO–LUMO gap, which should be valid for a gold–GMP–gold system, where the molecules interact only weakly with the electrodes). Thus, conduction electrons are forced to overcome an energy barrier exceeding 2 eV at the gold–molecule link, even at $V_b = 0.75$ V. Coherent tunnelling is naturally suspected to be present under such circumstances[22]. According to Simmons model, I scales linearly with V_b when the kinetic energy of field-accelerated electrons eV_b is negligibly small compared to the tunnelling barrier, where e is the electron charge[23,24]. The linear I_p–V_b characteristics are thus suggestive of electron tunnelling through GMPs with a single-molecule conductance of ~0.1 nS, which plausibly agrees with first-principle calculations[12].

Transverse field-induced electrostatic forces are anticipated to influence the trapping duration of nucleotides in the electrode nanogaps[19]. Contrary to expectation, however, I_p–t_d scatter plots (Fig. 3e) suggest no conspicuous correlation between t_d and V_b. Therefore, although the transverse field makes an important contribution to the electrical detection of single nucleotides, providing a well-defined I_p by screening out possible molecular conformations, we cannot expect to use it to control the duration of the translocation.

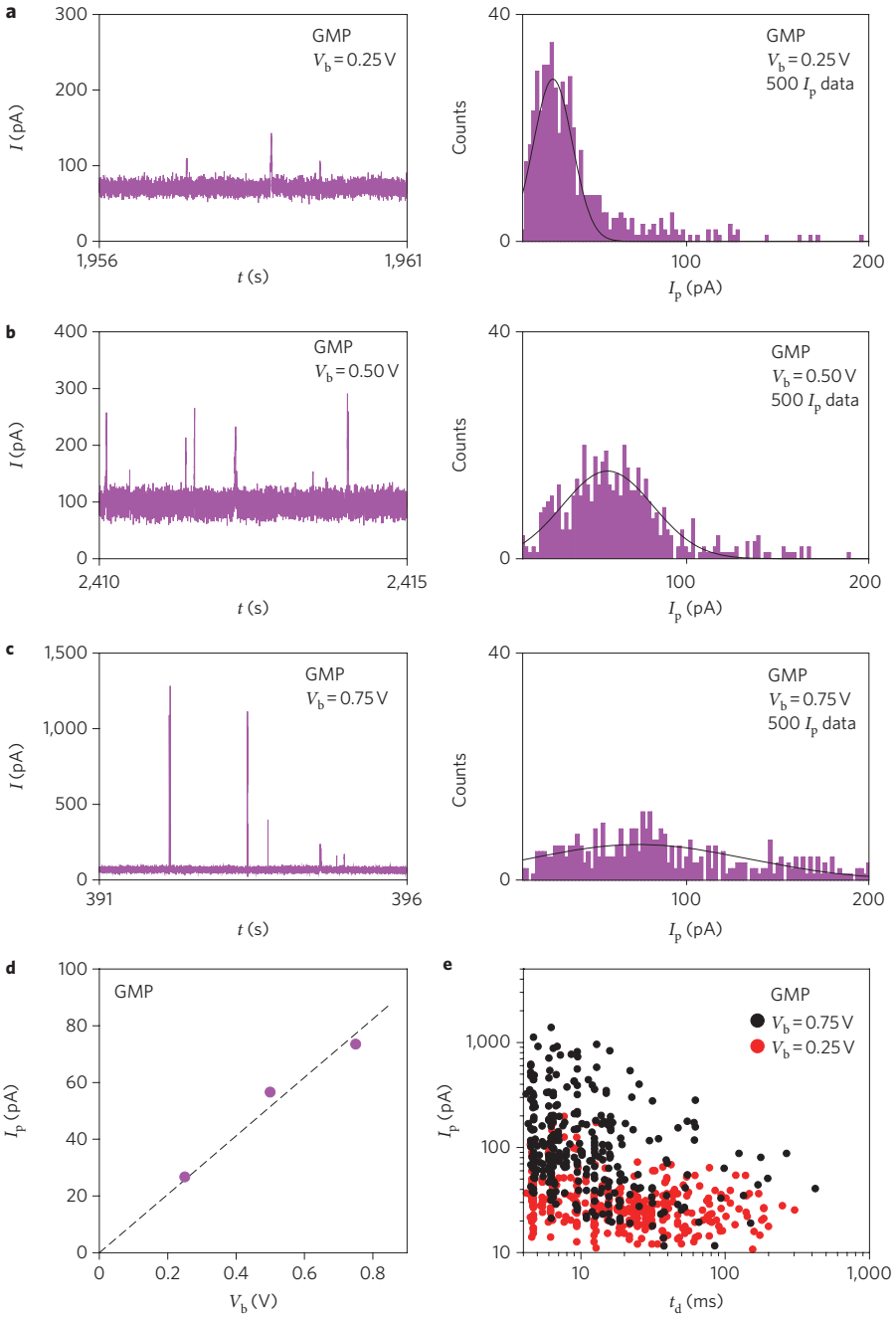

Figure 3 | I_p measurements for GMP conducted with V_b varying from 0.25 to 0.75 V, using a pair of nanoelectrodes with electrode gap size adjusted to 1.0 ± 0.05 nm. a–c, Partial I–t curves showing I pulses (left panels) and corresponding I_p histograms (right panels) acquired at $V_b = 0.25$ V (**a**), 0.50 V (**b**) and 0.75 V (**c**). Solid black lines are Gaussian fits to the histograms. I_p histograms reveal a single-peak structure. **d**, Plots of peak I_p extracted from each I_p histogram in **a–c** as a function of V_b. The broken line is a linear fit to the data. The linear I_p–V_b characteristics indicate electron tunnelling in single-nucleotide molecules. **e**, Scatter plots of I_p versus t_d. There is no obvious correlation between V_b and t_d.

Single-molecule measurements are also presented for the other nucleotides, that is, for TMP, CMP and adenosine 5′-monophosphate (AMP). AMP has rather complicated characteristics, with I–t curves demonstrating a high base level of current (>500 pA) and significant noise (Supplementary Fig. S4). These distinctive I–t characteristics are observed even when the electrode gap distance is extended to >2 nm. It is concluded that adenine shows a relatively high degree of non-specific binding to gold[25,26]. This peculiar affinity of adenines makes it difficult to avoid unintentional over-adsorption of AMPs on gold, thereby impeding the electrical detection of single-nucleotide molecules by means of I_p measurements.

It was, however, possible to observe the characteristic I pulses for the remaining nucleotides. Figure 4a displays I–t curves acquired for TMP and CMP at $V_b = 0.75$ V (results of GMP are also shown). The corresponding I_p histograms (Fig. 4b) have single peaks, suggesting effective transverse field effects that restrict molecular conformational freedom. The peak I_p values determine a single-molecule conductivity order of GMP > CMP > TMP. This result can be interpreted qualitatively as reflecting the order of differences in the DNA base HOMO–LUMO gaps of guanine < cytosine ≈ thymine[12,27], corroborating our assertion of electron tunnelling transport through single nucleotides.

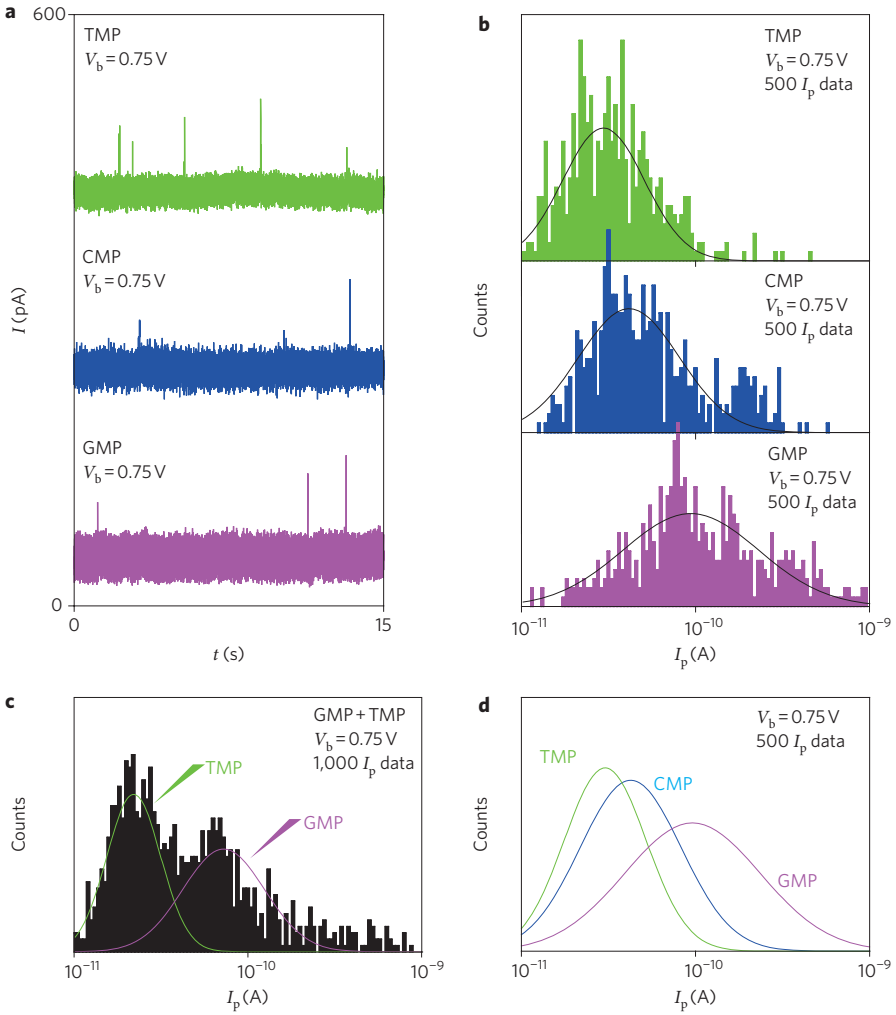

Figure 4 | Statistical identification of single nucleotides. a,**b**, Partial *I*–*t* curves obtained using a pair of nanoelectrodes with electrode gap size adjusted to 1.0±0.05 nm (**a**) and the corresponding I_p histograms of TMP (green), CMP (blue) and GMP (purple) (**b**). Solid lines are Gaussian fits to the histograms. **c**, I_p histogram obtained for a solution containing equimolar amounts (5 μM) of GMP and TMP. Electrode gap size, 1.0±0.05 nm. Solid curves are Gaussian fits, revealing two peaks of similar peak area. **d**, Superposition of single-nucleotide I_p distributions in **b**. The significant overlap of the histograms indicates the necessity of comparing statistical averages of the tunnelling current for identifying DNA sequences at the single-base level.

Single-nucleotide molecule identification is a key issue for DNA sequencing. In this context, we examined *I*–*t* measurements in a solution containing equimolar amounts of TMP and GMP. The resulting I_p histogram (Fig. 4c) reveals two distinct peaks ascribable to single-molecule conductance of TMP (green) and GMP (purple), thereby demonstrating that single nucleotides can be identified by means of two-probe tunnelling current detections.

A superposition of I_p histograms of GMP, CMP and TMP demonstrates considerable overlap (Fig. 4d), indicating that a single-shot measurement is certainly inadequate for identifying nucleotide types. This suggests a critical need to correct statistical averages of tunnelling current acquired over a period (with a high data sampling rate) for reading out a DNA base sequence while it translocates through an electrode nanogap[13]. Although such a single-molecule technique requires precise control of DNA dynamics in the vicinity of nanoelectrodes, a promising tool capable of manipulating the molecular translocations at the single-molecule level has already been developed[9,28].

Methods

Fabrications of nanoelectrodes. The first requisite for single nucleotide conductance measurements was to form a pair of electrodes with an inter-electrode gap spacing comparable to the molecular length of the nucleotides (~1 nm). We used nanofabricated mechanically controllable break junctions (nano-MCBJs) for this purpose, which combine excellent mechanical stability and high inter-electrode gap size controllability at a subpicometre resolution[19,29]. Fabrication procedures of nano-MCBJs are described elsewhere[20,29]. Gold nanoscale junctions were first pattered on a polyimide-coated flexible metal substrate using standard electron-beam lithography and lift-off techniques. Subsequently, polyimide lying under the junctions was etched away using a reactive ion etching process. The thus-fabricated gold nanobridges were stretched by bending the substrate in a three-point bending configuration to form a pair of nanoelectrodes.

Formation of 1-nm inter-electrode gaps. The gap spacing between a pair of electrodes formed by nano-MCBJs was controlled at a subpicometre resolution by finely manipulating the substrate deflection using a piezo-actuator. Precise control of the inter-electrode gap distance was implemented by taking full advantage of the self-breaking technique developed in our laboratory[20,30]. We elongated a gold nanojunction at a constant d.c. bias V_b with a serial resistor of 10 kΩ under a programmed junction stretching speed using a resistance feedback method[20,30]. This technique allows highly reproducible formation of nanoelectrodes with a gap distance narrowly distributed around 0.6±0.05 nm (ref. 20). The electrode gap distance was further configured to obtain nanoelectrodes with an inter-electrode gap distance precisely adjusted to the average length of the nucleotides (~1.0 nm). To accomplish this, we performed calibrations for electrode gap size control by examining the exponential decay of tunnelling current flowing through an electrode nanogap in relation to the gap distance in a vacuum in advance of any single-nucleotide detection measurements (Supplementary Fig. S2). After forming a well-defined nanogap, we carried out two-probe electrical detection of single-molecule nucleotides. All experiments are conducted at room temperature

in a nucleotide-dissolved Milli-Q (Millipore) solution (5 μM) under a flow of argon gas. The protonation state of the nucleotides was not controlled in this unbuffered solution, but this is unlikely to affect the electronic states of the π-bonded rings that dominate the tunnelling. Nucleotide molecules were purchased from Tokyo Chemical Industry Co. for GMP, TMP and CMP, and from Oriental Yeast Co. for AMP. We used ribonucleotides for adenine, guanine and cytosine to ensure easy handling and chemical and thermal stability of the molecules during the experiments, and used deoxyribonucleotide for thymine, because ribonucleotide monophosphates for thymine were not commercially available in the quantities necessary for carrying out the single-molecule detection measurements.

Tunnelling current measurements. For 1.0-nm inter-electrode gaps, tunnelling current I across the nanoelectrodes was amplified using a home-built logarithmic amplifier capable of reading picoampere currents at the level of 1×10^3 Hz, and the output signal was recorded at a sampling rate of 2 kHz using a 24-bit DAQ card (NI USB-9234, National Instruments). We performed I–t measurements over consecutive 50 min periods and, after each measurement, replaced each sample with a new one. Although it could be more convenient to reuse a MCBJ sample for more than one I–t measurement by simply reforming gold nanoelectrodes using the break junction technique, we chose to replace the entire sample to minimize possible contaminations. More than 20 MCBJ samples were used for each type of nucleotide to acquire 500 I-pulse signals.

Control experiments on single π-conjugated organic molecules. The reliability of the two-probe single-molecule detection method was verified by applying it to organic molecules other than nucleotides (Supplementary Figs S5,S6). We used three types of molecule: benzenedithiolates (BDTs), benzenediamines (BDAs) and benzeneamines (BAs). Electrical detection measurements were conducted by forming 0.7- or 0.5-nm electrode gaps in a dilute 1,2,4-trichlorobenzene solution (5 μM) of targeted molecules and monitor I–t curve evolutions. These molecules all demonstrated current ups and downs suggestive of single-molecule trapping and detrapping in the electrode gap nanospace. However, they showed a clear difference in the magnitude of the current rise I_r and the trapping duration t_d. I_r varied as BDT (∼100 nA) ≈ BDA (∼100 nA) ≫ BA (∼0.1 nA) whereas t_d varied as BDT (>1 s) > BDA (∼0.1 s) > BA (∼0.01 s). The observed characteristics can all be explained consistently by differences in the electronic coupling and chemical bonding strength at the molecule–electrode links, thereby validating the adequacy and accuracy of the electrical detection technique to probe electron transport of single nucleotides.

Received 27 October 2009; accepted 12 February 2010; published online 21 March 2010

References

1. Collins, F. S., Green, A. E., Guttmacher, A. E. & Guyer, M. S. A vision for the future of genomics research. *Nature* **422,** 835–847 (2003).
2. Schloss, J. A. How to get genomes at one ten-thousandth the cost. *Nature Biotechnol.* **26,** 1113–1115 (2008).
3. Dekker, C. Solid-state nanopores. *Nature Nanotech.* **2,** 209–215 (2007).
4. Branton, D. *et al.* The potential and challenges of nanopore sequencing. *Nature Biotechnol.* **26,** 1146–1153 (2008).
5. Zwolak, M. & Di Ventra, M. Colloquim: physical approaches to DNA sequencing and detection. *Rev. Mod. Phys.* **80,** 141–165 (2008).
6. Clarke, J. *et al.* Continuous base identification for single-molecule nanopore DNA sequencing. *Nature Nanotech.* **4,** 265–270 (2009).
7. Stoddart, D., Heron, A. J., Mikhailova, E., Maglia, G. & Bayley, H. Single-nucleotide discrimination in immobilized DNA oligonucleotides with a biological nanopore. *Proc. Natl Acad. Sci. USA* **106,** 7702–7707 (2009).
8. Fologea, D. *et al.* Detecting single stranded DNA with a solid state nanopore. *Nano Lett.* **5,** 1905–1909 (2005).
9. Keyser, U. F. *et al.* Direct force measurements on DNA in a solid-state nanopore. *Nature Phys.* **2,** 473–477 (2006).
10. Gershow, M. & Golovchenko, J. A. Recapturing and trapping single molecules with a solid-state nanopore. *Nature Nanotech.* **2,** 775–779 (2007).
11. van Dorp, S., Keyser, U. F., Dekker, N. H., Dekker, C. & Lemay, S. G. Origin of the electrophoretic force on DNA in solid-state nanopores. *Nature Phys.* **5,** 347–351 (2009).
12. Lagerqvist, J., Zwolak, M. & Di Ventra, M. Fast DNA sequencing via transverse electronic transport. *Nano Lett.* **6,** 779–782 (2006).
13. Lagerqvist, J., Zwolak, M. & Di Ventra, M. Influence of the environment and probes on rapid DNA sequencing via transverse electronic transport. *Biophys. J.* **93,** 2384–2390 (2007).
14. He, J., Lin, L., Zhang, P. & Lindsay, S. Identification of DNA basepairing via tunnel-current decay. *Nano Lett.* **7,** 3854–3858 (2007).
15. Chang, S. *et al.* Tunnelling readout of hydrogen-bonding-based recognition. *Nature Nanotech.* **4,** 297–301 (2009).
16. Fischbein, M. D. & Drndic, M. Sub-10 nm device fabrication in a transmission electron microscope. *Nano Lett.* **7,** 1329–1337 (2007).
17. Liang, X. & Chou, S. Y. Nanogap detector inside nanofluidic channel for real-time label-free DNA analysis. *Nano Lett.* **8,** 1472–1476 (2008).
18. Maleki, T., Mohammadi, S. & Ziaie, B. A nanofluidic channel with embedded transverse nanoelectrodes. *Nanotechnology* **20,** 105302 (2009).
19. Tsutsui, M., Taniguchi, M. & Kawai, T. Transverse field effects on DNA-sized particle dynamics. *Nano Lett.* **9,** 1659–1662 (2009).
20. Tsutsui, M., Taniguchi, M. & Kawai, T. Fabrication of 0.5 nm electrode gaps using self-breaking technique. *Appl. Phys. Lett.* **93,** 163115 (2008).
21. Frisch, M. J. *et al. Gaussian03, revisionC.02.* (Gaussian, Inc., 2003).
22. Troisi, A. & Ratner, M. A. Molecular signatures in the transport properties of molecular wire junctions: what makes a junction 'molecular'? *Small* **2,** 172–181 (2006).
23. Simmons, J. G. Generalized formula for the electronic tunnel effect between similar electrodes separated by a thin insulating film. *J. Appl. Phys.* **34,** 1793–1803 (1963).
24. Wang, W., Lee, T. & Reed, M. A. Mechanism of electron conduction in self-assembled alkanethiol monolayer devices. *Phys. Rev. B* **68,** 035416 (2003).
25. Kundu, J. *et al.* Adenine- and adenosine monophosphate (AMP)–gold binding interactions studied by surface-enhanced Raman and infrared spectroscopies. *J. Phys. Chem. C* **113,** 14390–14397 (2009).
26. Brown, K. A., Park, S. & Hamad-Schifferli, K. Nucleotide–surface interactions in DNA-modified Au–nanoparticle conjugates: sequence effects on reactivity and hybridization. *J. Phys. Chem. C* **112,** 7517–7521 (2008).
27. Taniguchi, M. & Kawai, T. DNA electronics. *Physica E* **33,** 1–12 (2006).
28. Peng, H. & Ling, X. S. Reverse DNA translocation through a solid-state nanopore by magnetic tweezers. *Nanotechnology* **20,** 185101 (2009).
29. Agraït, N., Yeyati, A. L. & van Ruitenbeek, J. M. Quantum properties of atomic-sized conductors. *Phys. Rep.* **377,** 81–279 (2003).
30. Tsutsui, M., Shoji, K., Taniguchi, M. & Kawai, T. Formation and self-breaking mechanism of stable atom-sized junctions. *Nano Lett.* **8,** 345–349 (2008).

Acknowledgements

This work was supported in part by the Grant-in-Aid for Scientific Research on Innovative Areas (no. 20200025) from the Japanese Ministry of Education, Culture, Sports, Science and Technology.

Author contributions

M. Taniguchi and T.K. planned and designed the experiments. M. Tsutsui, M. Taniguchi and K.Y. participated in fabrications of nano-MCBJs and single-nucleotide detection measurements. M. Tsutsui, M. Taniguchi and K.Y. performed data analyses. M. Tsutsui, M. Taniguchi and T.K. co-wrote the paper.

Additional information

The authors declare no competing financial interests. Supplementary information accompanies this paper at www.nature.com/naturenanotechnology. Reprints and permission information is available online at http://npg.nature.com/reprintsandpermissions/. Correspondence and requests for materials should be addressed to M.T. and T.K.